

2013

A murine model of aging-related neurodegeneration caused by a defect in DNA repair

<https://hdl.handle.net/2144/12098>

"Downloaded from OpenBU. Boston University's institutional repository."

BOSTON UNIVERSITY
SCHOOL OF MEDICINE

Thesis

**A MURINE MODEL OF AGING-RELATED NEURODEGENERATION
CAUSED BY A DEFECT IN DNA REPAIR**

by

KAITLIN FARRELL

B.S., University of Pittsburgh, 2011

Submitted in partial fulfillment of the
requirements for the degree of

Master of Arts

2013

Approved by

First Reader

Fernando Garcia-Diaz, Ph.D.
Associate Professor of Physiology & Biophysics

Second Reader

Laura Niedernhofer, M.D./Ph.D.
Associate Professor of Metabolism and Aging
The Scripps Research Institute, Florida

ACKNOWLEDGEMENTS

The guidance and direction of Dr. Niedernhofer and Dr. Beer-Stolz were invaluable to the completion of my thesis project.

**A MURINE MODEL OF AGING-RELATED NEURODEGENERATION
CAUSED BY A DEFECT IN DNA REPAIR**

KAITLIN FARRELL

Boston University School of Medicine, 2013

Major Professor: Fernando Garcia-Diaz, Ph.D., Associate Professor of
Physiology & Biophysics

Abstract

ERCC1 is a DNA repair protein that forms a heterodimer with XPF. The resultant dimer is active in multiple systems of DNA repair. Mutations in this repair mechanism result in progeroid syndromes, such as Xeroderma Pigmentosum. These syndromes present with progressive neurodegeneration and are modeled by deletion or transgenic knock down of the ERCC1 gene in mice. Global knockouts and *Ercc1*^{-Δ} mice, in which only 5% of the normal complement of ERCC1 is expressed, have been studied in order to elucidate the cause of the neural pathology. These models, similar to patients, often show neurodegeneration, but it was unclear whether this loss was due to a primary neuronal dysfunction or that of supporting glial cells. *L7Cre;Ercc1*^{-cond} mice, in which Ercc1-XPF is deleted only in the neurons of the forebrain, are used in this study to determine the cell autonomous impact of DNA repair deficiency on neurons. Oxidative damage is thought to contribute to the progression of aging-

related neurodegenerative disease, such as AD and PD, and DNA could be a prominent target. The hypothesis that pathology in *L7Ercc1^{-cond}* mice is similar to that of neurodegenerative disease states was supported in many instances. The decrease in weight seen in mutant mice is also seen in patients with both AD and PD. The degeneration in the hippocampus and alteration in DG proliferation is consistent with that often seen in AD, as is cortical degeneration and thinning of the corpus callosum. Gliosis in the striatum is seen in many PD patients and could be contributing to the ambulation impairment seen in the mutant mice. These data suggest a link between DNA repair deficiency and neurodegeneration stemming from multiple origins. Elucidating the impact of unrepaired endogenous DNA damage on neurons using this genetic tool may allow for the development of future interventions to slow aging-related neurodegeneration, as well as the progression of AD and PD.

Table of Contents

Title	i
Reader's Approval Page	ii
Acknowledgement	iii
Abstract	iv-v
Table of Contents	vi-vii
List of Figures	viii
List of Abbreviations	ix
Introduction	1-6
Methods	7-9
Mice	
Behavioral tests	
Immunohistochemistry	
Imaging	
Results	10-36
Phenotype overview	
Body weight	
Ambulation assessment	
Inflammation response	
Cell death assay	
Cellular characterization	
Discussion	37-41

List of Journal Abbreviations	42
References	43-46
VITA	47-49

LIST OF FIGURES

Figure	Title	Page
1	ERCC1-XPF dimer	4
2	Oxidation in ERCC1- Δ	4
3	Peripheral neuropathy in ERCC1- Δ	5
4	Phenotype overview	11
5	Body weight, survival	12- 13
6	Balance and Coordination	14
7	GFAP hippocampus	16-17
8	TUNEL hippocampus	18
9	Nissl hippocampus	20- 22
10	Ki-67 hippocampus	24
11	Ki-67 GFAP hippocampus	25
12	BRDU hippocampus	27-28
13	Nissl corpus callosum	30-31
14	GFAP corpus callosum	32-33
15	GFAP cortex and striatum	34
16	TUNEL substantia nigra	35-36

ABBREVIATIONS

AD	Alzheimer's disease
CC	Corpus callosum
CX	Cortex
DG	Dentate gyrus
PD	Parkinson's disease
SN	Substantia Nigra
STR	Striatum
TH	Tyrosine Hydroxylase
XP	Xeroderma Pigmentosum

Introduction

Aging is frequently associated with the risk of developing neurodegenerative diseases, such as Parkinson's disease (PD) and Alzheimer's disease (AD) (Eller et al. 2001, Kaup et al. 2011). AD is characterized by memory impairment associated with volume loss in regions such as the hippocampus (Kaup et al., 2011). PD is characterized by a loss of dopaminergic neurons in the substantia nigra, resulting in motor impairment and dysfunction, such as tremor (Braak et al., 2002). Successful cognitive aging in the absence of neurodegenerative disease is positively correlated with the volume of certain brain structures (Kaup et al., 2011). Global brain volume is positively correlated with overall cognition, while hippocampal volume is associated with memory function. This would suggest that a decrease in cell number is a crucial factor in cognitive decline (Kaup et al., 2011). Oxidative damage is one current theory about the cause of cell loss and cognitive/memory dysfunction commonly associated with aging. Hamilton et al. (2001) showed a correlation with age and increased oxidative DNA damage in multiple strains of rodents. DNA damage is also causal to the pathologies in DNA repair deficiency syndromes, such as xeroderma pigmentosum (XP) and ataxia telangiectasia, which include progressive neurological degeneration (Borgesius et al. 2011, McNeil et al. 2012). Given the link between cell loss and DNA damage in aging and disease states such as XP, characterization of the effects of this damage on neurons may contribute to treatment intervention in the future. Murine models of DNA repair

deficiency syndromes provide a unique opportunity to elucidate the effect of DNA damage on brain structures and function.

ERCC1

Ercc1 is a DNA repair protein involved in nucleotide excision repair, interstrand crosslink repair, and double-strand break repair (Niedernhofer et al., 2004). *Ercc1* dimerizes with the protein XPF to interact with DNA (figure 1) (McNeil et al., 2012, Tsodikov et al., 2005). *Ercc1* and XPF are found in a mutated form in nucleotide excision repair disorders such as XP, resulting in sensitivity to UV damage, as well as endogenous DNA damage (McNeil et al., 2012). The *Ercc1*^{-/-} murine model is used to characterize the effects of DNA repair deficiency in a premature aging system (McWhir et al. 1993). These mice, however, age so quickly that their lifespan is reduced to only approximately 4 weeks (Nevedomskaya et al., 2010, Niedernhofer et al., 2006). *Ercc1*^{-Δ} mice have some protein function remaining, slowing the progression of aging. Analysis of neural pathology in these mice demonstrates increased glial response throughout many areas of the brain (de Waard et al., 2010). Preliminary data generated by the Greenamyre lab suggest that in the substantia nigra region of *Ercc1*^{-Δ} mice, such reactive gliosis is present, consistent with neurodegeneration and increased oxidative stress, but no frank loss of dopaminergic neurons (figure 2). Although the absence of cell loss is a different pathological manifestation than that characteristic of PD, these data suggest that there is neural injury, nonetheless. This implies a possible underlying link between DNA repair

deficiency and neurodegenerative disease. There is also a decrease in the size and an irregularity in the shape of nerve fibers in the *Ercc1*^{-Δ} model, as demonstrated by Goss et al. (2011) (Figure 3). Other neuronal pathologies found in *Ercc1*^{-Δ} mice include degeneration in motor neurons of the spinal cord, Purkinje cells of the cerebellum, hippocampal neurons and axons of fiber tracts, such as the corpus callosum (Borgesius et al., 2011, de Graaf et al., 2013, de Waard et al., 2010). The symptomatology in the substantia nigra and the peripheral nervous system could account for the ambulation impairment seen in these mice. Although there are marked neural alterations throughout the brain, *Ercc1*^{-Δ} mice develop symptoms spanning multiple organs, including kidney and liver impairments (Dolle et al. 2006, Nevedomskaya et al., 2010). The *Ercc1*^{-cond} mice utilized in this study (*L7Ercc1*^{-cond}) have mutations limited to neurons of the forebrain in order to more narrowly characterize the importance of DNA repair to cognition. We hypothesize that there will be degeneration in brain structures that are also commonly affected by neurodegenerative disease states such as AD and PD.

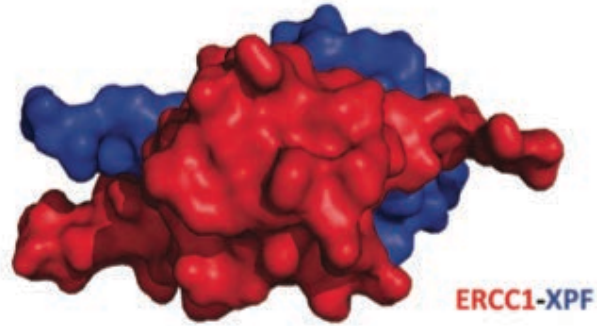


Figure 1 taken from McNeil et al. 2012: Three-dimensional model of helix-hairpin-helix configuration in the ERCC1-XPF dimer

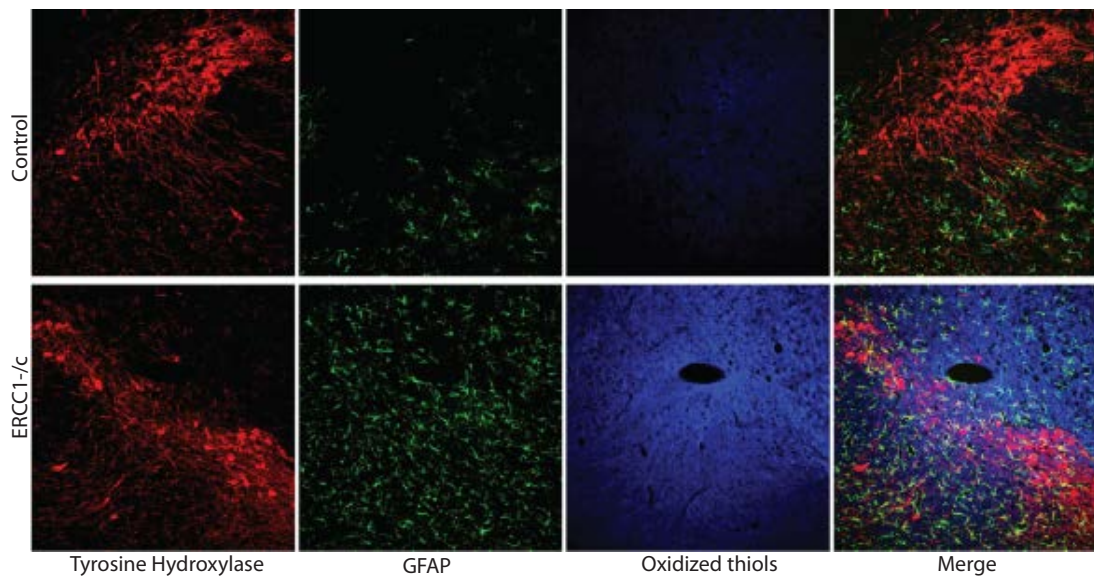


Figure 2 . Work from the lab of Dr. Greenamyre demonstrating increased oxidation (blue) in the ERCC1 Δ mice. An increase in GFAP (green) is also seen. The presence of characteristic TH stain (red) confirms that the affected area is the substantia nigra.

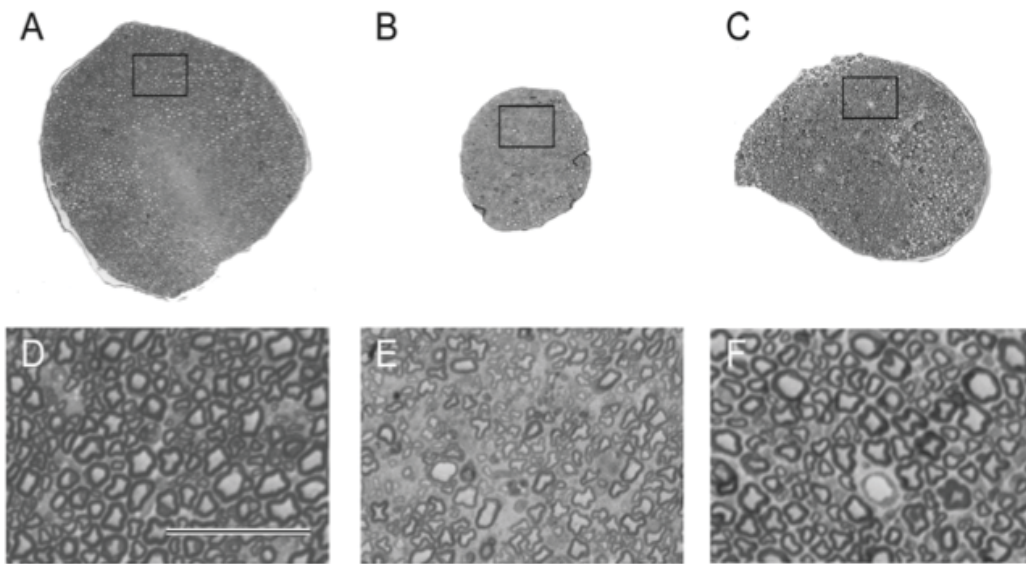


Figure 3 adapted from Goss et al, 2011. Micrographs depict the crosssection of the sciatic nerve in a 20 week control mouse (A), a 20 week *Ercc1*- Δ mouse (B), and a 120 week old control mouse (C). D, E, and F are magnified images of the boxed area in the cross-sections above. The 20 week old *Ercc1*- Δ mouse has a significant decrease in the thickness of individual nerve fibers and an irregularity in shape when compared to a control mouse of the same age. This phenotype is similar to, but more exaggerated than that seen in an aged control mouse.

Objectives

Although previous studies in mice and humans have demonstrated that deficiency of Ercc1-XPF DNA repair endonuclease has a profound effect on the nervous system, it is not clear what the mechanism of neurodegeneration is. Using transgenic mice in which only neurons are lacking Ercc1-XPF activity, the objectives of this study are:

- 1) To determine if the animals suffer from a primary neurodegeneration, i.e., if loss of neurons is a cell-autonomous event.
- 2) To determine which areas of the brain are affected by DNA repair deficiency, which will reveal which neurons are hypersensitive to oxidative DNA damage.
- 3) To characterize cellular changes in the neurons of these areas
- 4) To compare and contrast these changes with age-related degenerative diseases

If these goals are accomplished, it will establish a link between endogenous DNA damage and neurodegeneration that may be pertinent to common age-related CNS diseases. The mechanism of neurodegeneration in inherited DNA repair deficiency syndromes will also be elucidated. This lays the groundwork for developing rationale strategies for disease treatment or prevention in the future

Methods

Mice

Mice were housed in the animal facility of Hillman Cancer Center UPMC and given food and water ad libitum. The Division of Laboratory Animal Research guidelines and IACUC approved protocols were utilized.

Brains were analyzed from *CamKII α -Cre;Ercc1^{-/cond} (L7Ercc1^{-/cond})* and control littermate mice at 2.5 months, 9.5 months, 10 months, and 11.7 months for Ki-67 staining, a marker of cell proliferation. Five mutant mice and five controls were assessed (one of each genotype at each age point). For GFAP, TH and nissl stain, ten *L7Ercc1^{-/cond}* and ten control littermate mice were analyzed (one of each genotype at 2.5, 9, 9.5, 10.3, 11, 11.7, and 13.7 months. two of each genotype were analyzed at 10 months. One mouse of each genotype at 2 months of age was used to assess cell death). An early time point was used in order to assess cell death before much of the degeneration had already occurred.

Behavioral Tests

Motor coordination was tested using the rotarod system. Mice were given a week of training on the system in order to decrease anxiety. Animals were tested weekly thereafter. A speed of 15 revolutions per minute was used. The time to fall was recorded.

Immunohistochemistry

Brains were fixed in 4% paraformaldehyde and subsequently cryoprotected in a solution of 30% sucrose. Brains were then cryosectioned and placed in wells of 1x PBS with 0.2% azide until further processing. Floating sections were prepared for immunostaining by blocking for 1 hour at room temperature in a solution of 5% normal donkey serum in 1% triton PBS. Tissues were then incubated in primary antibody (diluted in 5% normal donkey serum in 1% triton PBS) at 4°C overnight, washed in 1% triton PBS, 1xPBS, and subsequently incubated in secondary antibody (diluted in 1% normal donkey serum in 1% triton PBS) for 1 hour at room temperature. After washes in 1x PBS, tissues were mounted onto slides and coverslipped via fluormount. Primary antibodies used include tyrosine hydroxylase (TH, ab9702, 1:250), ki-67 (ab9260, 1:350), and glial acidic fibrillary protein (GFAP, ab4674, 1:350). Secondary antibodies include d-light 488, cy3 and cy5.

BrdU

One *L7Ercc1*^{-/cond} mouse and one control mouse at 3 months of age were injected for one week with BrdU. Brains were dissected, flash frozen and subsequently cryosectioned in a sequential manner onto superfrost plus slides and stored at -20°C. Tissues were fixed for 15 minutes in 2% paraformaldehyde and subsequently stained for BrdU expression. After fixation, tissues were washed in PBS and incubated for 15 minutes in 0.1% triton PBS. Tissues were washed in PBS and blocked in 2% BSA for 45 minute. After washes in 0.5% BSA tissues were incubated in anti-BrdU at 1:250 dilution for 1 hour at room

temperature. Subsequent washes in 0.5% BSA were carried out and then tissues were incubated in secondary for 1 hour at room temperature. Tissues were washed in 0.5% BSA and then 1x PBS and hoecht stain applied. After final washes, tissues were coverslipped with gelvatol.

TUNEL Assay

To detect cell death a roche TUNEL assay kit was used. After initial washes with 1x PBS, cells were incubated in TUNEL mixture for 20 minutes and room temperature. This mixture consisted of 90ul of dH₂O, 64ul of TdT buffer, 40ul CoCl₂, 2ul TdT, and 2 ul biotin. Tissues were then washed with 1xPBS and streptavidin cy3 antibody was applied for 30 minutes at room temperature. After washes with 1x PBS tissues were coverslipped with gelvatol.

Nissl Stain

Tissues were serially hydrated via 3-minute washes in 100% ethanol, xylenes, 100% ethanol, 70% ethanol, and 20% ethanol. Tissues were then washed for 5 minutes in dH₂O and subsequently incubated in 0.1% cresyl violet solution for 5 minutes. After washes in dH₂O, tissues were serially dehydrated via 20% ethanol, 100% ethanol and xylenes.

Imaging

Slides were analyzed via the Nikon 90i upright tiling scope. Images were taken at 20x magnification and stitched to create larger views. Images were analyzed via Nikon elements software.

Results

Phenotype Overview

Figure 4 demonstrates some key phenotypic features of the *L7Ercc1*^{-/cond} mutant mice. At around 8.5 months, mutant mice exhibit compulsive scratching of the head and ears to the point of self-mutilation, causing open wounds on the neck region, apparent in figure 4A and 4C. The cerebral atrophy caused by the *Ercc1* mutation at 10 months is evident in Figure 4B and in the middle images of Figure 4C. Stars in Figure 4C mark the regions that clearly elucidate cortical shrinkage in mutant mice, revealing the midbrain. It appears that the cerebellums of these mice are not atrophied, which is to be expected due to normal *Ercc1* expression in this structure.

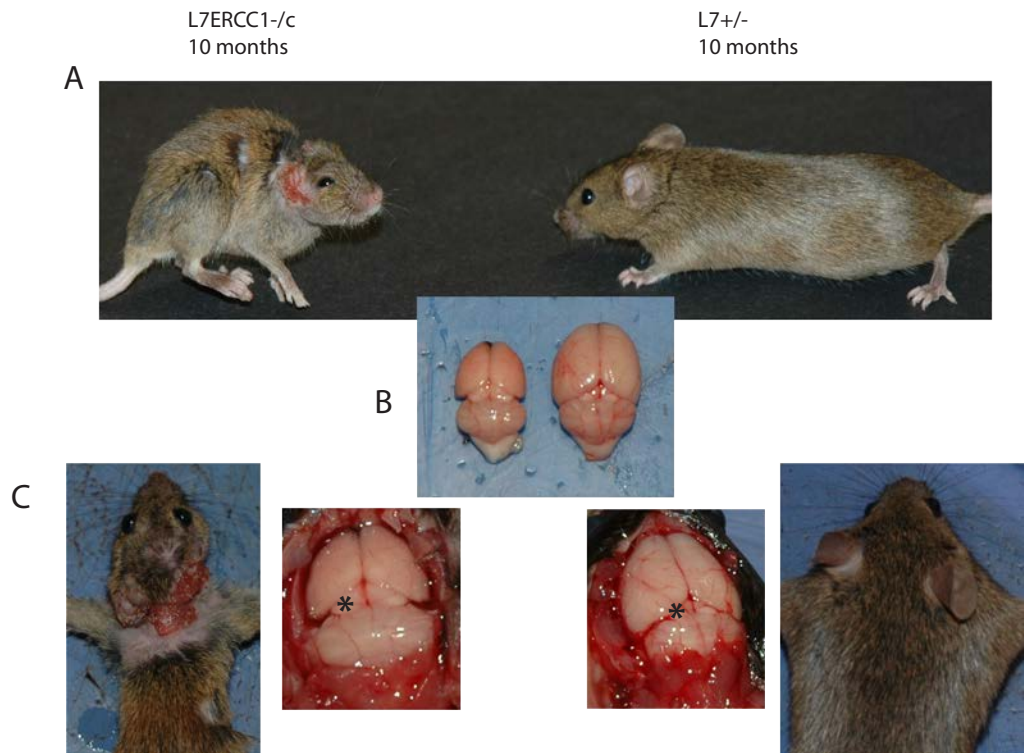


Figure 4 . A) Images demonstrate obsessive scratching, causing the open wounds visible on mutant mice. B) Brain of mutant mouse (left)and control mouse (right) of the same age demonstrate the decrease in size of the mutant brains. This size decrease is seen significantly in the cortex (star- midbrain is more visible in mutant mouse due to cortical atrophy). C) Far left image further depicts the scratch wounds mutant mice inflict on themselves. Middle images show mutant brain (left) and control brain (right) of the same age inside of skull to further demonstrate cortical atrophy.

Body Weight

A graph of the body weights of mutant mice compared to littermate controls across time shows that at 8 months, the mutants start to lose weight (Figure 5a). These controls include mice that are heterozygous for Ercc1 expression, as they do not present with a phenotype. This weight loss increases with age, becoming lowest at 10 months. This symptom presents around the time neural changes become evident.

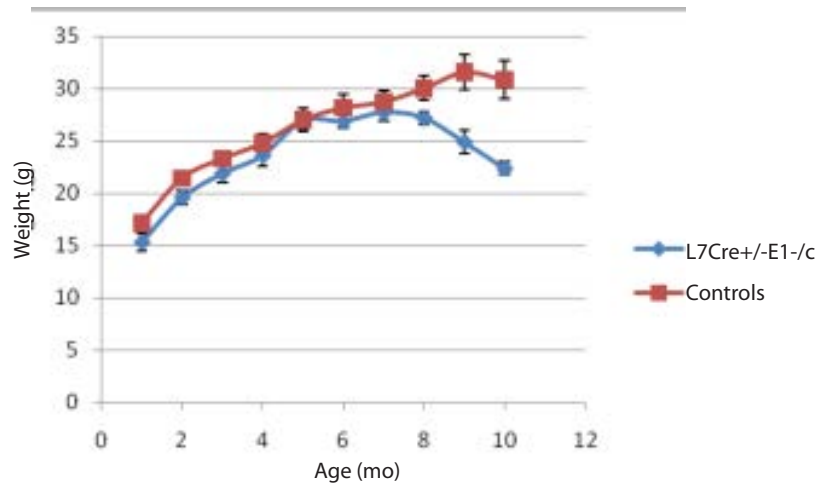


Figure 5a: Graph demonstrates weights of L7 mice compared to littermates, including ERCC1+/- mice.

Survival

A decrease in survival percentage was seen in mutant mice at approximately 5 months of age and progressed steadily to the point of zero survival, around 18 months. Control mice do not begin to decline in survival until after 16 months and maintain above a 50% survival percentage at 18 months (Figure 15b).

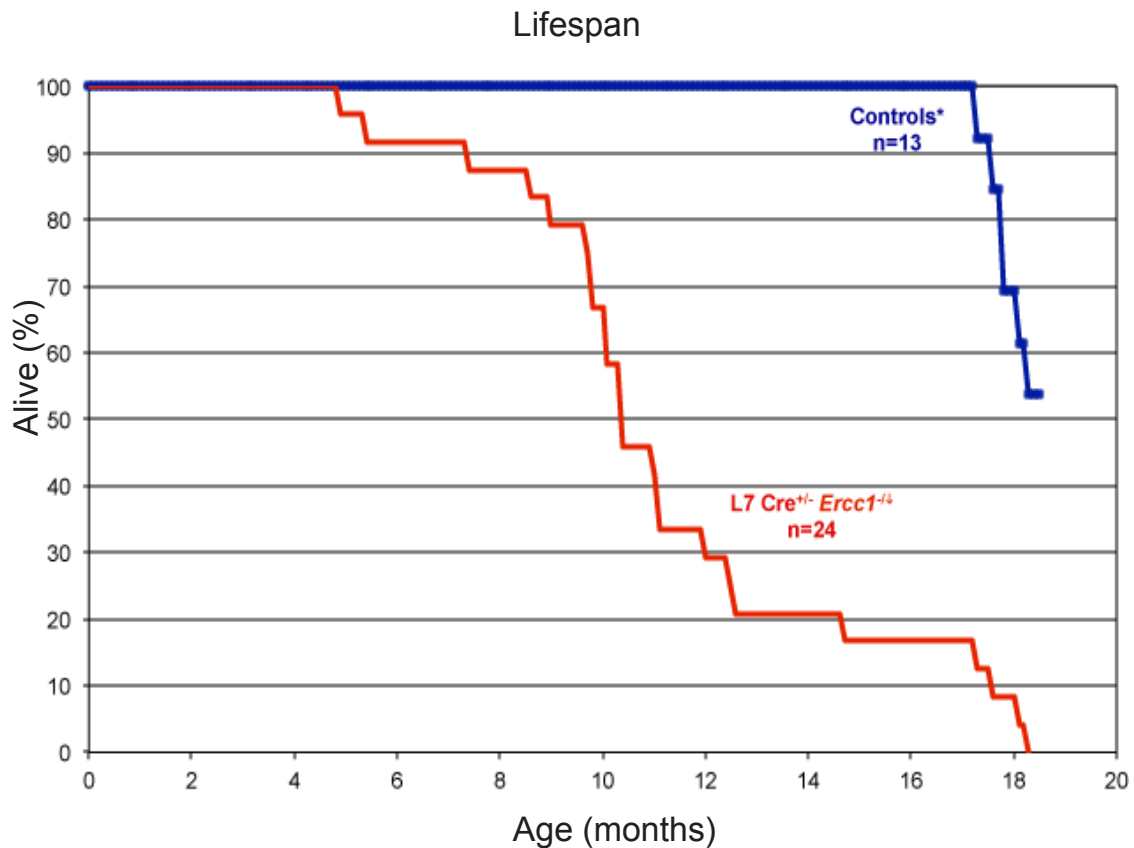


Figure 5b. Graph demonstrates survival percentages of L7ERCC1^{-/-} mice (red, n=24) versus controls (blue, n=13). A clear decrease in survival percentage is seen in mutant mice around age 5 mo and steadily declines. Controls do not start to decrease in survival until after age 16 mo. At survival percentage of zero for mutant mice, above 50% of controls remain.

Balance and Coordination

Ambulation was assessed using the rotarod system. Young mutant mice have comparable ambulation ability to control mice (Figure 6B), implied by similar time spent on the rotarod. However, older *L7Ercc1^{-/cond}* mice (>6mo) have an impaired ability to maintain balance and coordination on the rotarod system (Figure 6A, B).

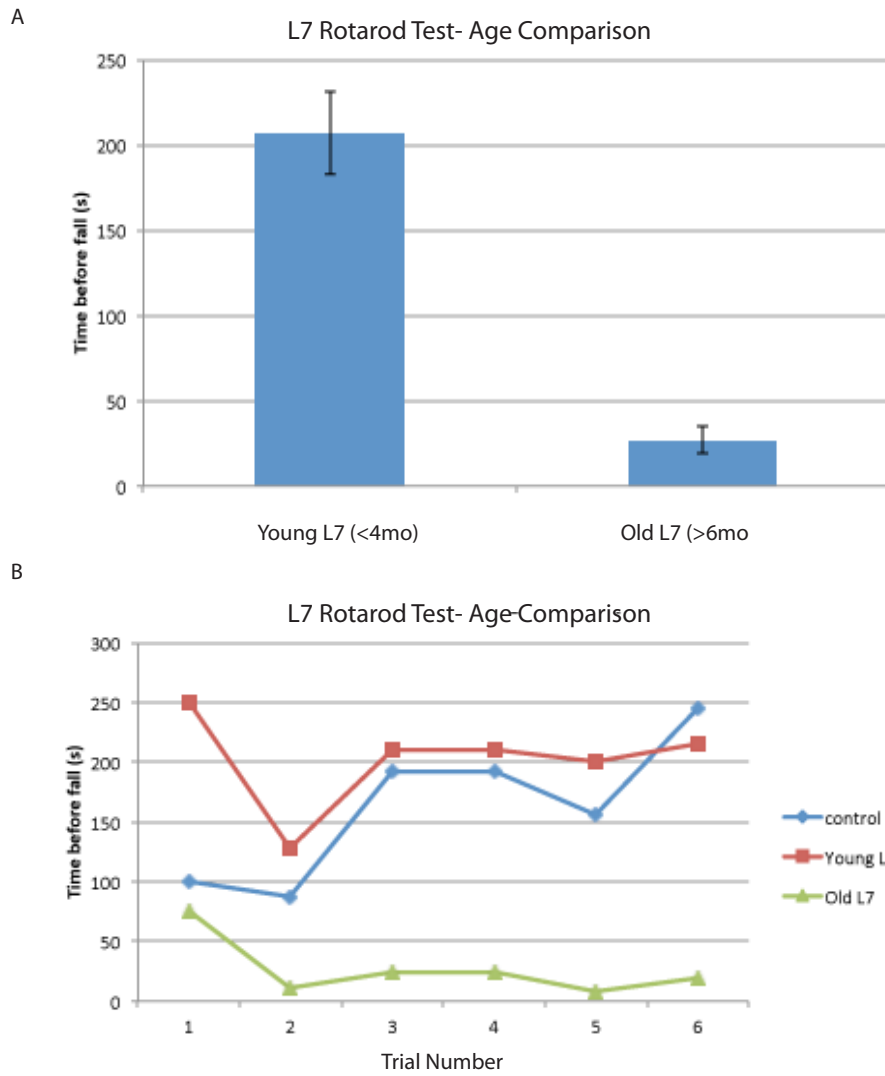


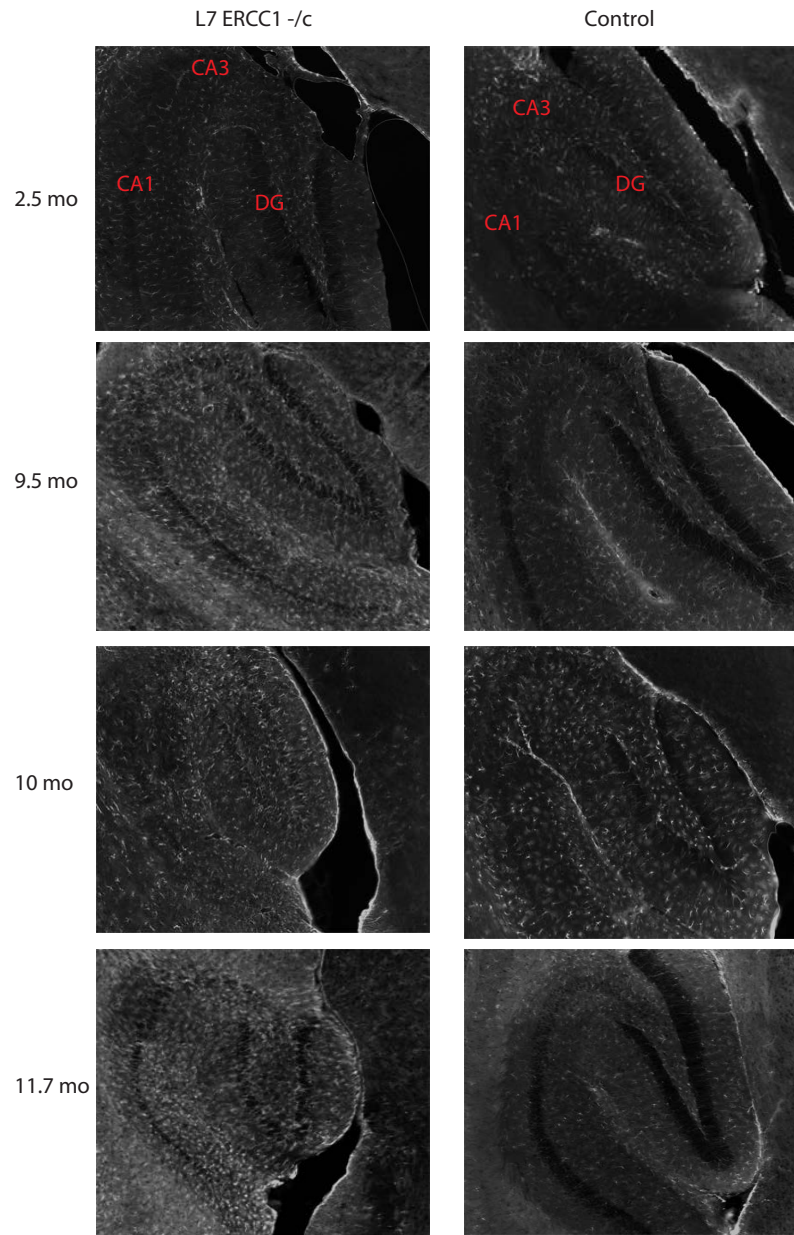
Figure 6. A) Bar graph demonstrates a significant decrease in the time coordinated movement can be maintained on the rotarod by old mutant mice (>6mo, n=2) compared to young mice of the same genotype (<4 mo, n=5). B) Line graph demonstrates similar performance between young mutant mice (red) and control mice (blue, n=5). However, a significant decrease in ambulation is demonstrated by old mutant mice (green).

Hippocampus

Glial Response

In order to localize inflammatory response to neural damage, tissues were stained with GFAP. *L7Ercc1*^{-/cond} and control mice had a comparable level of gliosis in the hippocampus at 2.5 months of age. At 9.5 months and on, an increased level of GFAP staining was seen in the hippocampal region of mutant mice when compared to control mice (Figure 7A). Zoomed image of GFAP in Figure 7B more clearly demonstrates this glial response in the CA1, CA3 and dentate gyrus. Although images were taken at the same magnification, neurodegeneration in the mutant hippocampus makes more of the structure visible in the field of view when compared to control mice. These data suggest that hippocampal neurons are susceptible to damage when DNA repair is deficient.

A



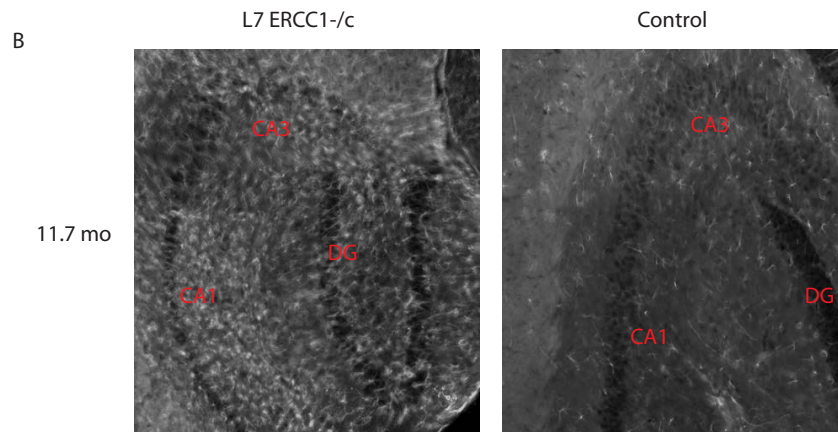


Figure 7) 20x A) GFAP staining shows an increase in glial cells in mutant mice after age 2.5 months in the hippocampus. B) zoomed image shows glial staining increase more clearly

Cell Death Assay

TUNEL assay signal, measuring fragmented DNA, appears higher in the CA1, CA3 and dentate gyrus regions (stars mark areas of interest) of mutant mice at 2.5 months of age (Figure 8). Although there is some signal in the control mice, there is a higher intensity and more punctate staining in the mutant mice, indicating higher cell death. The highest level of cell death appears to be in the dentate gyrus (DG). These results are cohesive with the neural damage

suggested by the increased in GFAP signal in the region.

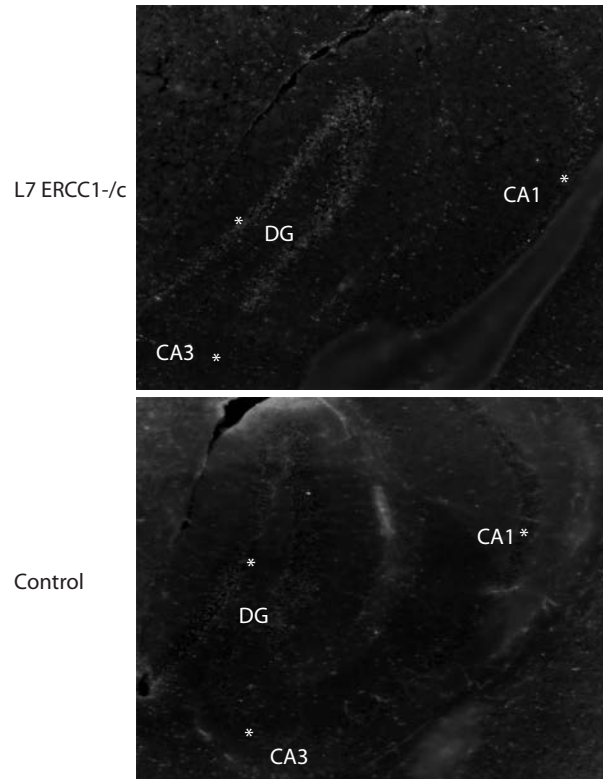


Figure 8. TUNEL stain in the hippocampus is more intense in the regions of interest (stars) in the mutant mice compared to controls.

Cellular characterization

In order to characterize neuronal shape and number, tissues were stained with nissl. Further cellular characterization was accomplished through BrdU staining and other immunohistochemical assessments.

A decrease in cell density was seen in the CA1 and CA3 regions after the 2.5-month time point in mutant mice (Figure 9A, B). At 11.7 months, the

degeneration in the mutant mice appears to spread to the dentate gyrus (DG) (Figure 9A, C). This cell loss is consistent with increased gliosis seen after 2.5 months in mutant mice.

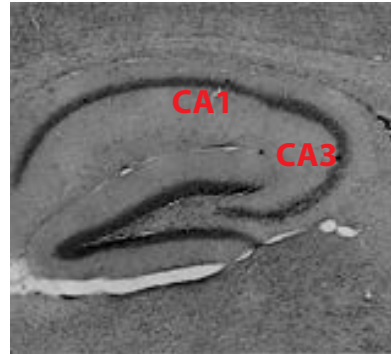
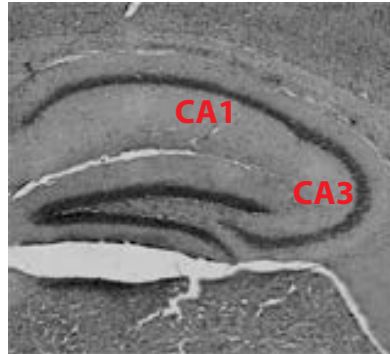
Enlarged cells, which are likely dying neurons, were seen beneath the subgranular zone of the DG in these mice as well. Because this region is home to the progenitor cells of the hippocampal formation, tissues were stained with Ki-67 to assess proliferation levels.

A

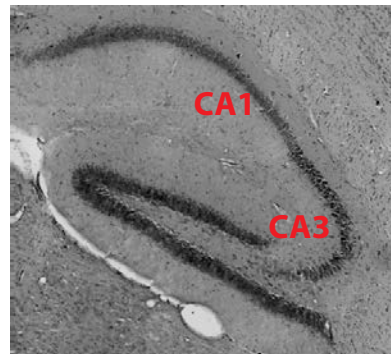
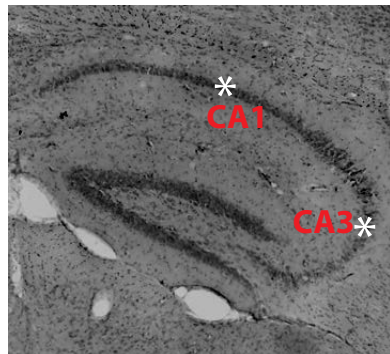
L7 ERCC1 ^{-/-}c

control

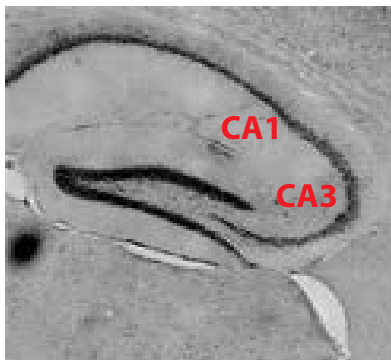
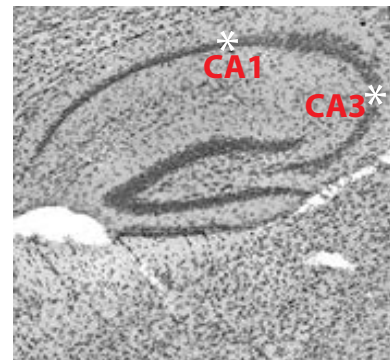
2.5 mo



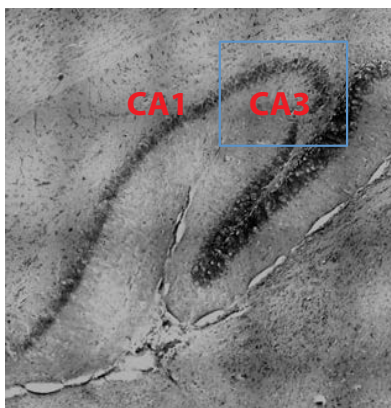
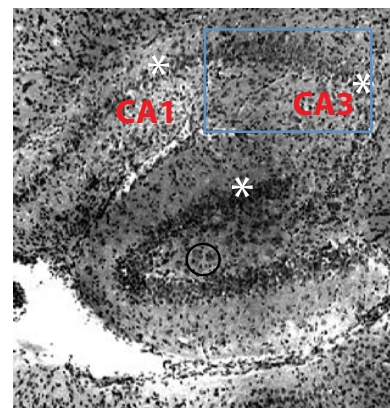
9.5 mo



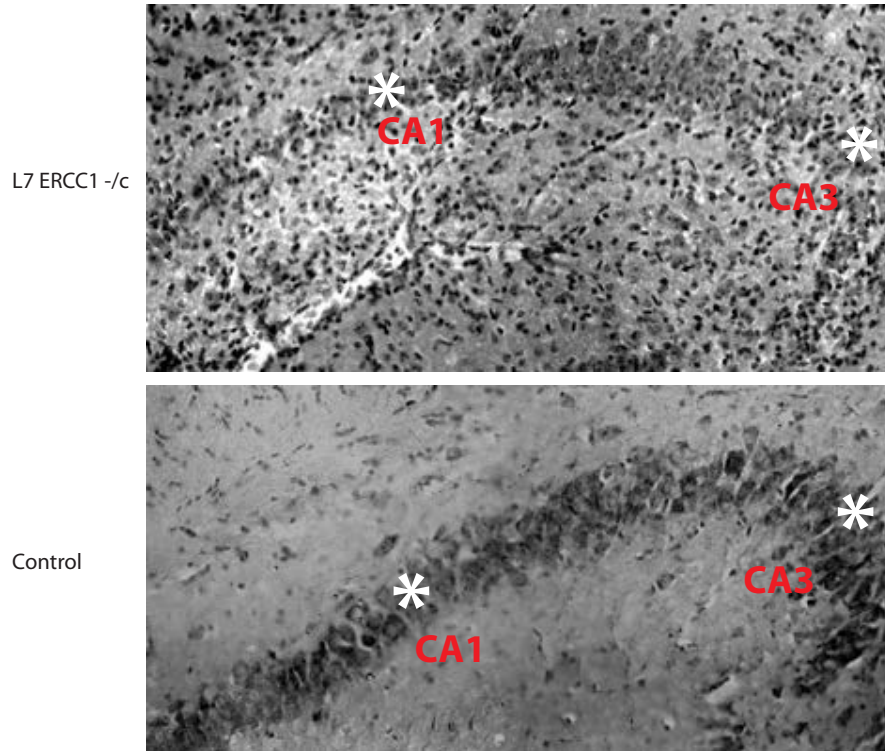
10mo



11.7 mo



B



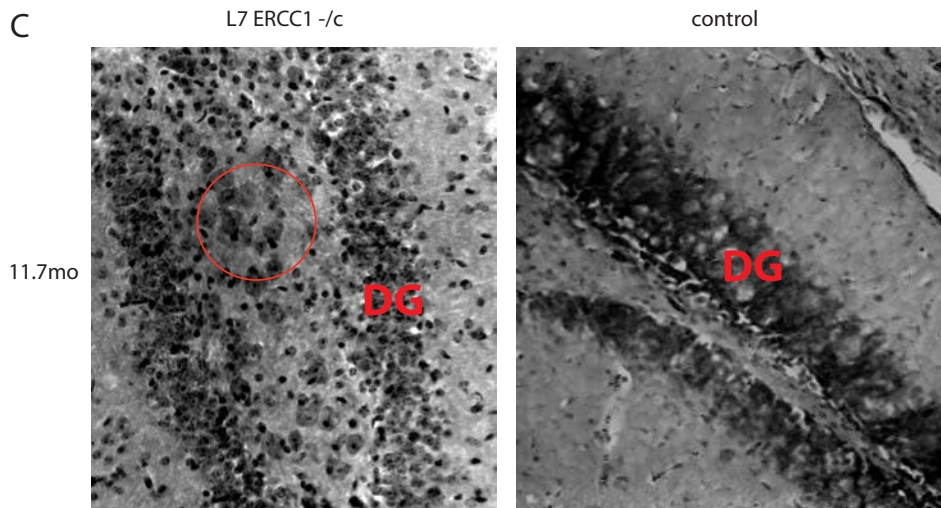


Figure 9. A) Nissl stain shows that after 2.5 months of age there is decrease in the cellularity of the CA1 and CA3 regions of the hippocampus in mutant mice (*). Swollen cells appear in the subgranular layer of mutant mice with increasing age as well (circle). B) A zoomed image of the CA1 and CA3 regions in mice of 11.7 months further demonstrates this cell loss in mutant mice (*). C) Zoomed image depicts swollen cells inside the dentate gyrus in mutant mice at 11.7 months.

At 2.5 months of age, proliferation in the two genotypes appears to be comparable (figure 10). However, with increasing age, Ki-67 signal seems to escalate in the mutant mice. In order to assess whether this increase in signal could be due to compensation for the degeneration in mutant mice or due to glial proliferation in response to neural injury, Ki-67 was combined with GFAP staining (figure 11). The signal overlay does not appear to show Ki-67 directly overlapping with GFAP. However, Ki-67 signal appears to become unspecific in the mutant mice with increasing age. This unspecific signal is frequently high in the region beneath the subgranular zone, in which the nissl demonstrated enlarged neurons (Figure 9C). This suggests that the extensive neurodegeneration seen in the

mutant mice may be the cause of unspecific Ki-67 labeling. In order to attain more specific labeling, BrdU injections were given to one mutant and one control mouse as described previously and the brain tissue was subsequently stained for BrdU.

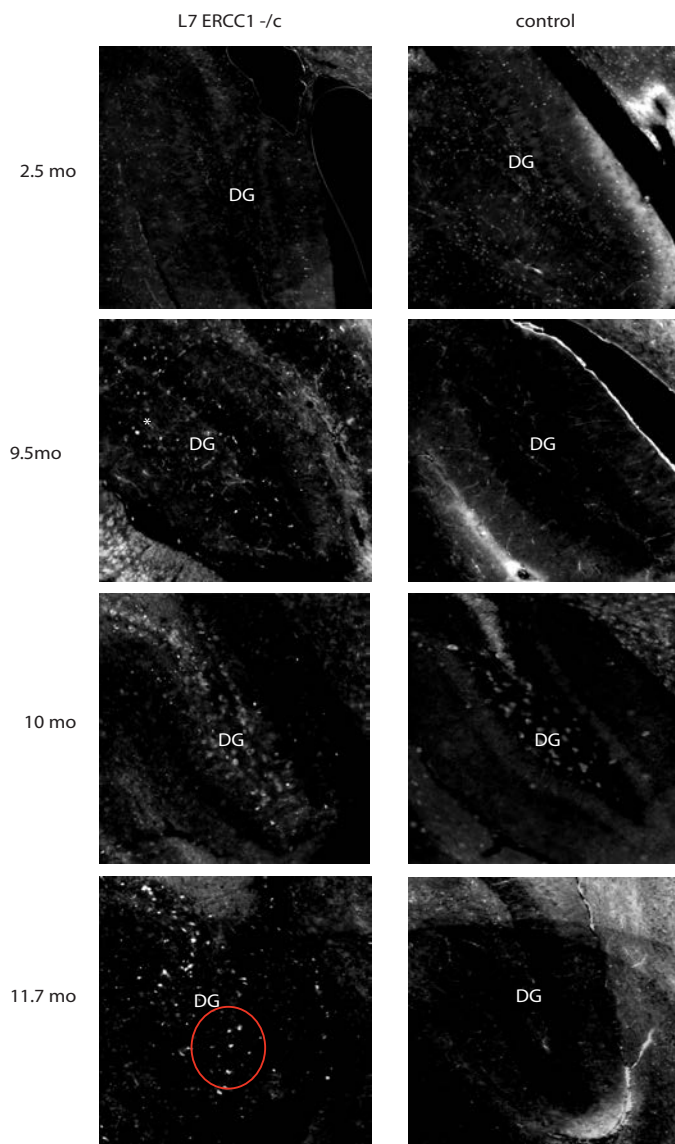


Figure 10. ki-67 staining demonstrates that at 2.5 months, proliferation is comparable between the two genotypes. After that time point the ki-67 stain appears to become less specific, especially in the mutant mice. Much of the unspecific staining seems to be labeling the neurons that coincide with the swollen neurons seen in the dentate gyrus via nissl stain (circle).

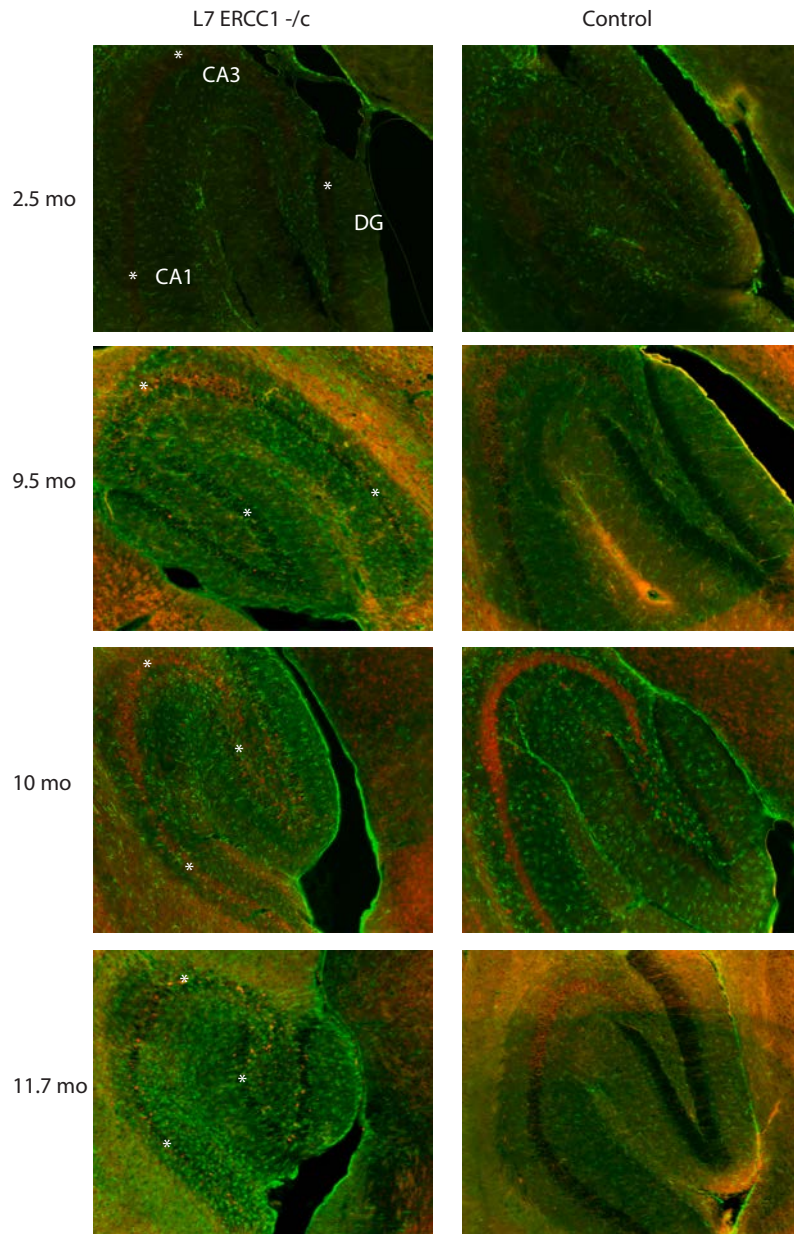
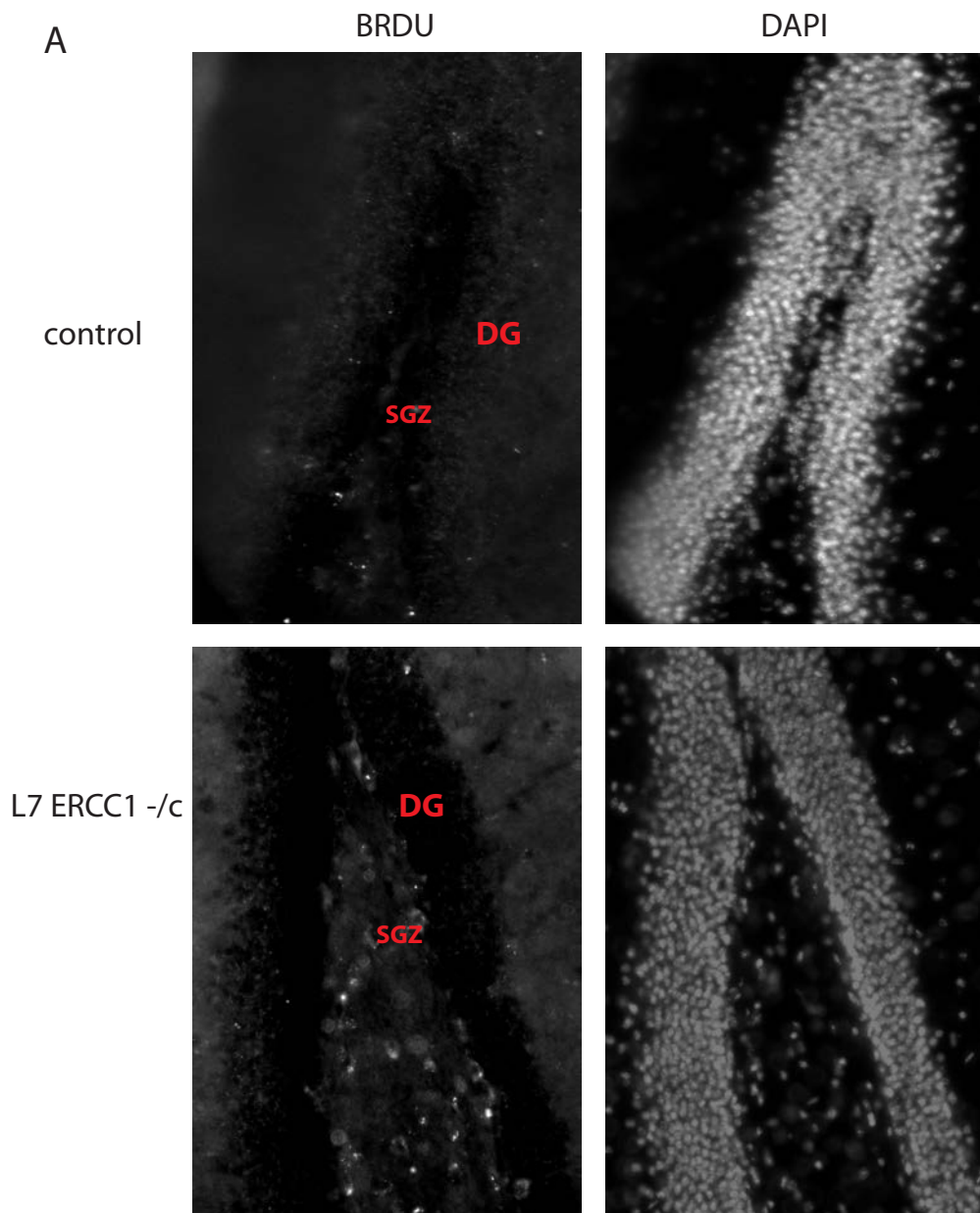


Figure 11. GFAP (green) and ki-67 (red) overlap shows no direct relationship between the unspecific ki-67 signal and an increase in glia (stars mark points of higher ki-67 signal in the regions of interest).

The BrdU signal appeared to be similar in the subgranular zone, home of the hippocampal progenitor cells, of the mutant mouse compared to control mouse at 3 months (Figure 12A). This finding indicates similar neurogenesis in the two genotypes at a young age. Due to the length of the injection period, BrdU signal could be expected in the granular layer of the DG due to migration of the newly proliferated cells from the subgranular layer. In this layer, however, the signal is almost negligible in the mutant when compared to the control mouse. This suggests that the proliferated cells in the hippocampus of *L7Ercc1^{-/cond}* mice degenerate before or shortly after replacing the current neurons in the DG and, therefore, cannot be located with BrdU staining. A higher magnification image of the DG (Figure 12B) shows that there is less overlap (purple signal, exemplified in square regions) between BrdU (red) and DAPI (blue) in the mutant than in the control mouse. The continued death of the newly proliferated cells could contribute to the decrease in cell number seen in the DG of older mutant mice.



B

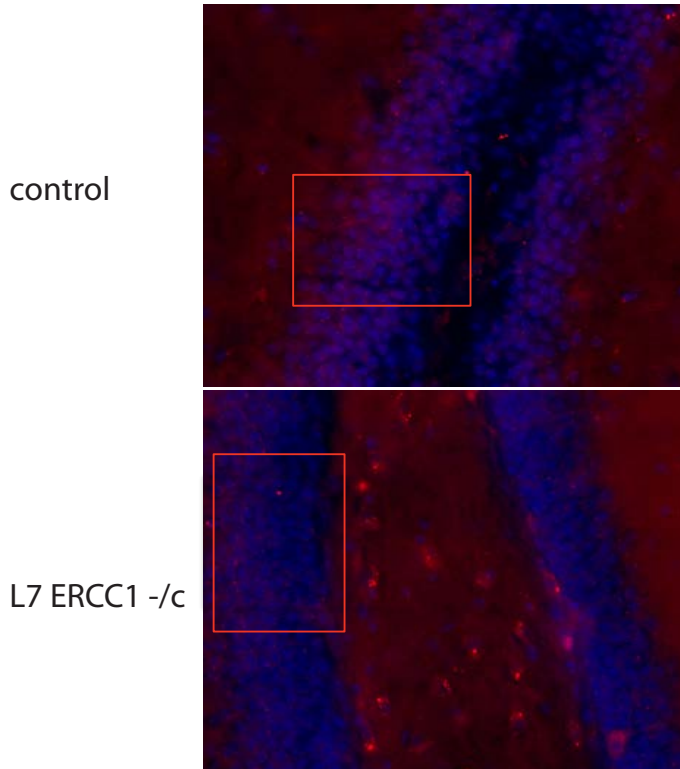


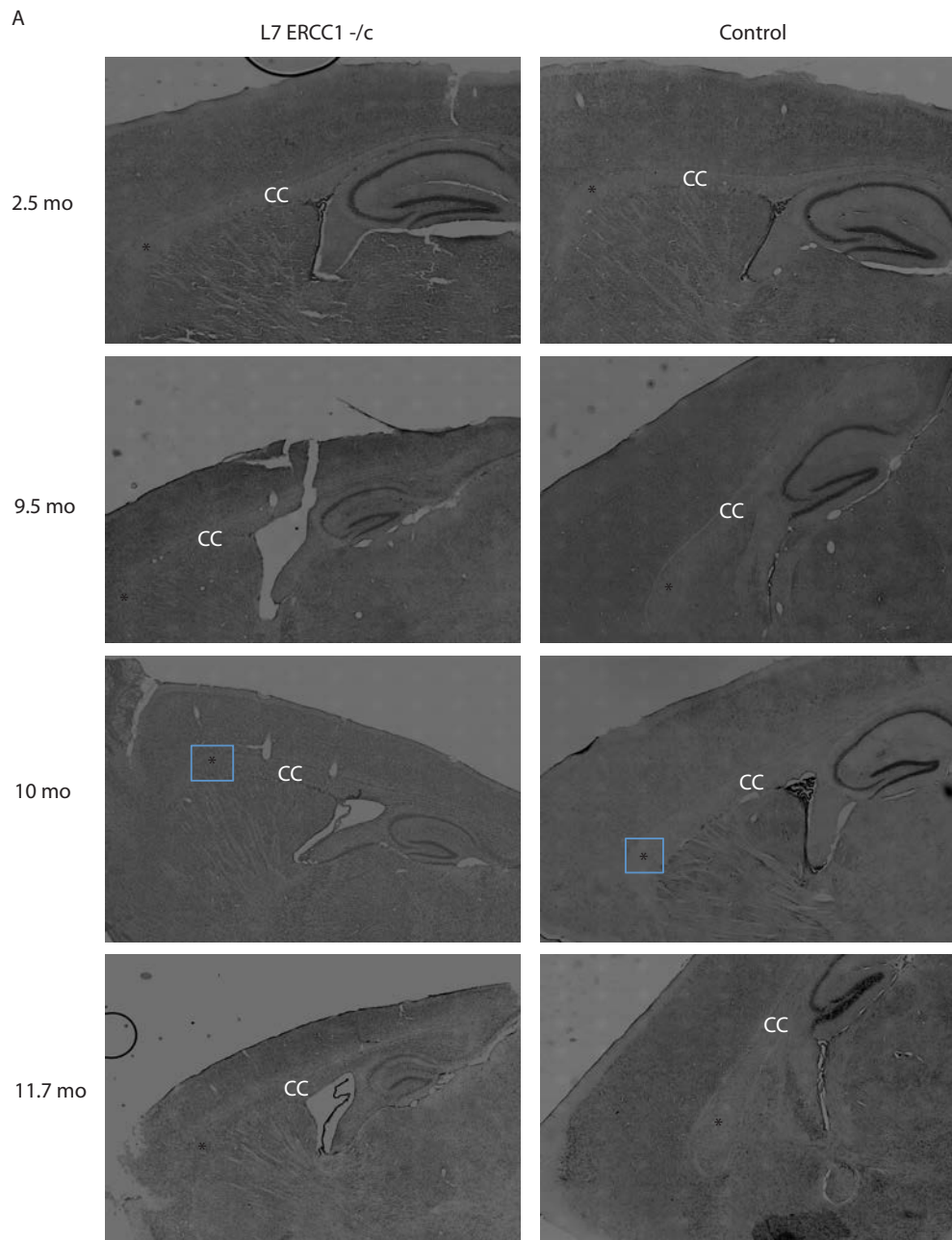
Figure 12. A) 20x, BRDU staining shows an increase in proliferation in cells of the control hippocampus. There is also a decrease in the proliferated cells traveling to the dentate gyrus in the mutant mice. B) 40x image more clearly shows higher overlap of BRDU (red) with DAPI (blue) confirming higher nuclear stain in control mice (square demonstrates region of overlap).

Corpus Callosum

Cellular Characterization

At the age of 2.5 months, the thickness of the corpus callosum as measured via nissl stain did not differ significantly between the two genotypes. However, at 9.5 months, the corpus callosum of the mutant mice appears to have a decreased fiber density compared to control mice (figure 13A). The borders of the corpus callosum are also less evident, making the fiber tract less recognizable in older mutants. The degeneration in the corpus callosum is

progressive, as the appearance of the corpus callosum is severely altered in 11.7 month-old *L7Ercc1*^{-/cond} mice when compared to controls of the same age (figure 13A). In addition to thinning of the tract, there appears to be an increase in cellularity of the corpus callosum in these mice compared to control mice. The increase appears most dramatic at or beyond 10 months of age (Figure 13B). GFAP staining suggests this may be due to a glial response in the area due to degeneration (Figure 14A). Gliosis appears to be most dramatic at the 11.7-month stage (Figure 14B). This inflammation is consistent with the atrophy seen at this time point in mutant mice.



B

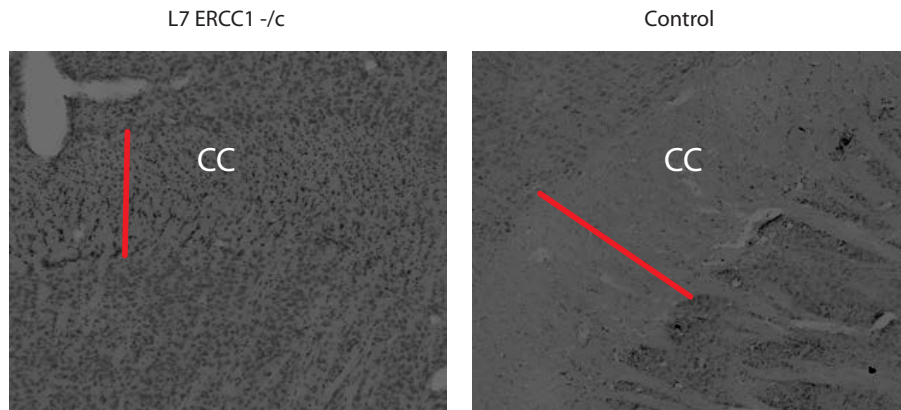
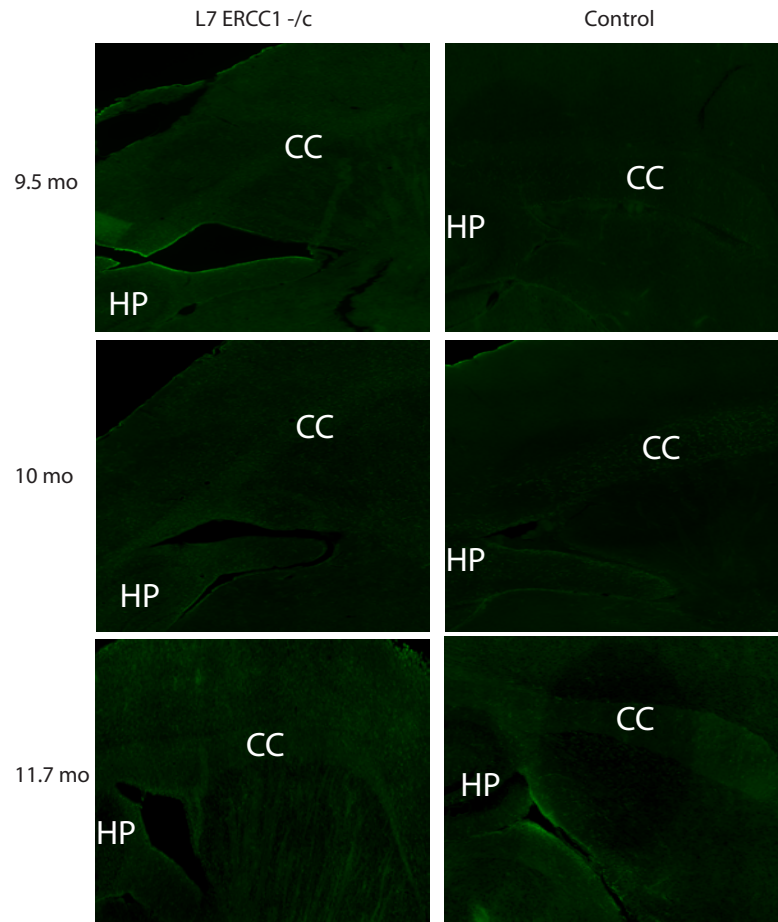


Figure 13. A) Nissl stain of the corpus callosum demonstrates thinning of the tract occurs in mutants after age 2.5 months. Zoomed area (squares) are shown in B. The zoomed image shows an increase in cellular labeling (dark puncta) and a decrease in thickness (red lines) in the mutant mice. This increase appears to be most dramatic after 9.5 months.

A



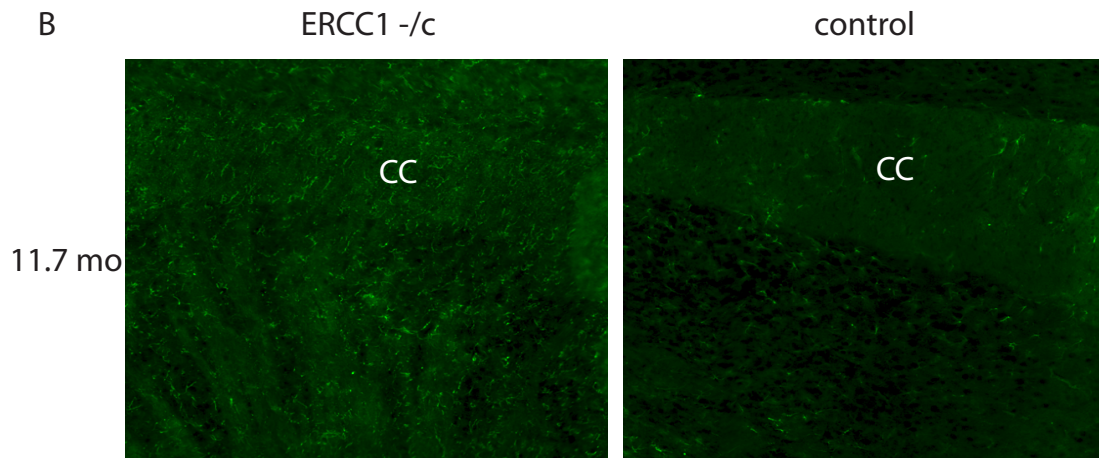


Figure 14. 20x A) Immunohistochemistry demonstrates an increase in GFAP in the corpus callosum in mutant mice 9.5 months and after. B) zoomed image of GFAP staining more clearly demonstrates the increase in the corpus callosum of mutant mice.

Cortex and Striatum

Inflammation response

Analysis of GFAP staining shows an increase in glia in the cortex and striatum of $L7Ercc1^{-/cond}$ mice (Figure 15). This increase was most apparent at 10 months and older.

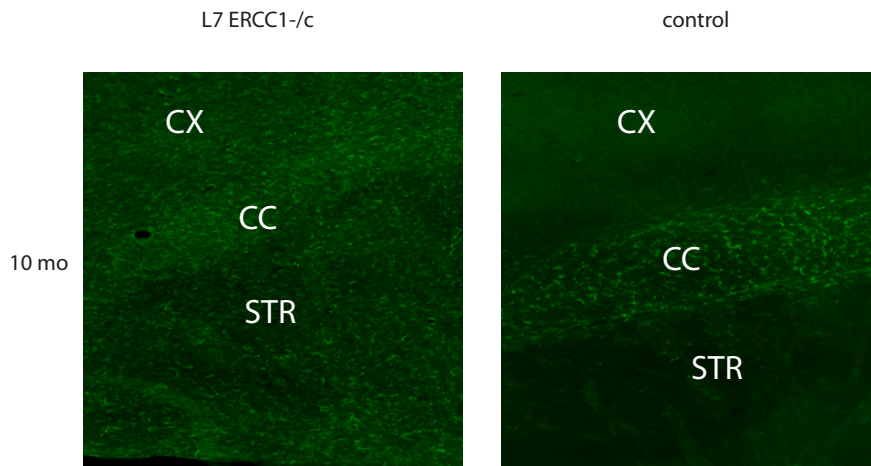


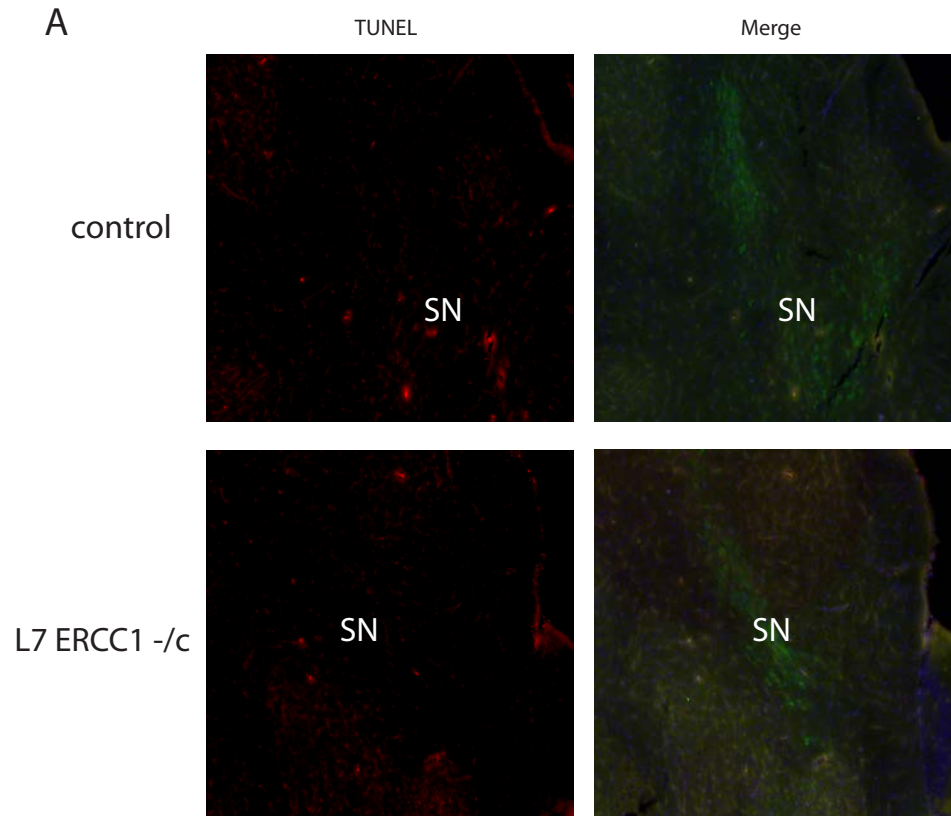
Figure 15. 20x image of GFAP staining in 10 mo mice demonstrates an increase in glial response in mutant mice when compared to controls.

Substantia Nigra

Cell death assay

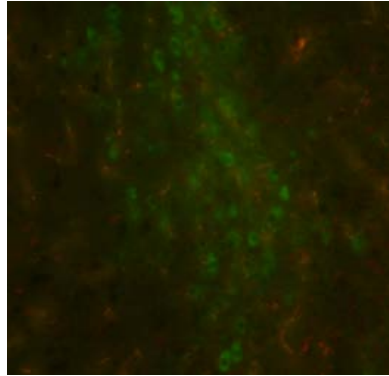
TUNEL assay in the substantia nigra at age 2.5 months (Figure 16) shows no overlap in either mutant or control mice with the TH neurons of the substantia nigra. TH is utilized to ensure accuracy of location to the presence of the protein in dopaminergic neurons. Figure 16B more clearly demonstrates lack of colocalization between the two signals. Although there appear to be less TH neurons in the mutant mice, this is likely a plane-of-section phenomenon. These

data suggest that at 2.5 months, there is no cell death in the substantia nigra.



B

Control



L7 ERCC1 $-/-$ c

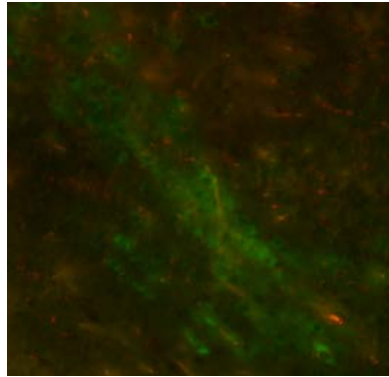


Figure 16. A) 20x Images demonstrate that there is no TUNEL stain (red) that colocalizes with the nuclei of TH neurons (green) in the substantia nigra. Although there are less TH neurons in the mutant mouse in this image, this is likely a plane-of-section phenomenon. B) Zoomed image of the substantia nigra smore clearly shows lack of overlap between the nuclear TUNEL stain (red) and TH (green).

Discussion

Ercc1 mutation leads to a progressive decrease in weight in mice starting at 8 months of age (Figure 5). Because the Ercc1 mutation is limited to neurons in the model being testing, it is unlikely that this weight loss is caused by primary dysfunction in the gastrointestinal epithelia. Weight loss is frequently a symptom in PD and AD as well (Zussy et al. 2013, Secher et al. 2012, Chen et al. 2003). This suggests that similar systemic effects occur in these neurodegenerative disease states and that of DNA repair deficiency, supporting the hypothesis previously presented.

Macroscopic cortical pathology in *L7Ercc1^{-/cond}* mice is evident at approximately 10 months of age. Reactive gliosis often occurs in response to such neural injury (Glass et al., 2010). Therefore, increased GFAP staining seen in the hippocampus suggests that there is similar degeneration in this structure. The presence of degeneration is supported by a decrease in the cellularity of the CA1, CA3 and dentate gyrus regions seen via nissl stain in mutant mice. It is likely that memory function is significantly decreased in these mice, similar to that seen in AD.

Degeneration in the hippocampus was again confirmed by an increase in TUNEL assay signal in *L7Ercc1^{-/cond}* mice, highest in the DG. The decreased cellularity is likely not caused by a lack of adult neurogenesis via progenitor cells in the subgranular layer, as suggested by a comparable BrdU signal in this region in both mutant and control mice. The neuronal degeneration in the DG

occurring at 11.7 months may be a result of the loss of the newly proliferated cells. It is possible that replacement of the DG neurons by neurogenesis is sufficient to prevent an obvious cell loss in that area until the degeneration becomes more extensive with age. Lack of BrdU signal in the granular layer of mutant mice, however, would suggest that his proliferation level is below that of significant immunohistochemical detection.

The decreased cellularity in the hippocampus of *L7Ercc1^{-/cond}* mice is similar to the degeneration seen in AD. The hippocampal proliferation effects, however, are currently variable among AD models and patients. Some studies demonstrate a decrease in proliferation with AD, while others show an increase (Jin et al., 2004, Lazarov and Marr, 2010, Winner et al., 2011). It is possible that the increase in proliferation signal in the latter studies is a result of glial response to the neurodegeneration (Winner et al., 2011). The increase in proliferation could also be explained by neural compensation to the degeneration (Winner et al., 2011. Jin et al., 2004). It is likely that the second scenario is the cause of the increased proliferation in the *L7Ercc1* mutant mice, as the GFAP staining does not colocalize with the ki-67 signal. Despite the uncertainty, similarities in the hippocampal degeneration in our model to that in AD pathology may suggest a link between DNA repair deficiency and cell loss in neurodegenerative diseases.

In addition to the hippocampus, pathology was seen in the corpus callosum of *L7Ercc1^{-/cond}* mice. This fiber pathway is crucial for communication between hemispheres of the brain, significant in the connection of cortical neurons (Teipel

et al., 2002). The *L7Ercc1* mutant mice show a thinning of this tract, likely due to degeneration of axons from cortical neurons. The mutant mice also show an increased cellularity in the corpus callosum. It is possible that the reactive gliosis that occurs in response to neurodegeneration, as demonstrated by an increased in GFAP staining, is the cause of this increase. The corpus callosum is quite often affected in many patients with AD as well, manifested as a thinning of the tract (Alves et al., 2012, Teipel et al. 2002). This phenomenon supports the hypothesis previously suggested and provides another link between DNA repair and common neurodegenerative disease pathologies.

Degeneration in the corpus callosum has been linked to the level of cortical degeneration in certain studies of AD (Teipel et al., 2002). This association is supported in the pathology of our model, given the large decrease in cortical brain mass seen in mutant mice at a macroscopic level. The glial response in the cortical region of *L7Ercc1*^{-/cond} mice is consistent with cortical injury as well. Cortical degeneration is another link between the pathologies of DNA repair deficiency and that of neurodegenerative diseases. There is often cortical thinning in patients with AD (Becker et al., 2011, Grand'Maison et al., 2013, Chang et al., 2013). Grand'Maison et al. (2013) demonstrated that this thinning could also be correlated with susceptibility to subsequent amyloid-B deposition.

L7Ercc1^{-/cond} mutant mice had impairment in ambulation when tested via rotarod. Although similar dysfunction is seen in PD models, it is predominantly caused by neuronal loss in the substantia nigra. The degeneration in this disease

is thought primarily to be a result of the presence of Lewy bodies in the dopaminergic neurons. However, it has been suggested that reactive oxygen species contribute to its progression (Ghosh et al., 2012, Ghosh et al., 2009). The L7Ercc1 mutant mice did not appear to have degeneration in the substantia nigra, as suggested by an absence of TUNEL stain colocalizing with the TH stain of the structure. The presence of oxidative damage in global Ercc1 transgenic mice (*Ercc1*^{-Δ} mice)(Figure 2), however, suggests that if a TUNEL stain were performed on tissues from older mice the results may show increased cell death. This possibility is currently being explored. Given that the *Ercc1*^{-Δ} mice also have peripheral neuropathy (Goss et al., 2011), it will be necessary to analyze nerve fibers in the *L7Ercc1*^{-cond} mice as an appropriate control.

The nigro-striatal circuit is also crucial for regular ambulation (Pradhan et al. 2013). The increase in GFAP signal in the striatum of mutant mice could contribute to the ambulation phenotype in the absence of substantia nigra degeneration. Neuroinflammation is seen in the striatum of many PD patients in addition to that in the substantia nigra, providing another link between pathologies due to DNA repair deficiency and those of neurodegenerative disease states (Gerhard et al., 2006, McGeer et al., 1988). It is thought that the neuroinflammation commonly associated with neurodegenerative disease states such as AD and PD actually impedes neural recovery (Pradhan et al. 2013

The hypothesis that DNA repair deficiency would cause pathology in the structures often affected in neurodegenerative disease states, such as AD and

PD, was supported in many instances during analysis. The hypothesis is not currently supported when analyzing degeneration in the substantia nigra of the mutant mice; however this neuronal death may be seen in older mutant mice. Given the many parallels between the patterns of degeneration in DNA repair deficient mice and that seen in PD and AD, it would be interesting to further elucidate the role of DNA repair in these patients. Future experiments include quantifying the cell loss in the hippocampus and additional characterization of the proliferation in mutant mice via BrdU injections. TEM analysis is also being performed on various regions of interest in mutant and control mice, which will elucidate ultrastructural changes due to DNA repair. Another interesting facet of this project to explore will be determining the root of the obsessive scratching.

The results of this study suggest that a repair deficiency could be facilitating the degeneration of neurons in common neurodegenerative disease systems. If confirmed, this fact could present a point for intervention- an opportunity to attempt the retardation of degeneration in these patients through the expression of Ercc1. The link between repair deficiency and neurodegeneration is an area that will likely provide interesting data for future studies.

LIST of JOURNAL ABBREVIATIONS

Ann. Neurol.	Annals of Neurology
Arch. Neurol.	Archives of Neurology
Exp. Neurol.	Experimental Neurology
Int. J. Geriatr. Psychiatry	International Journal of Geriatric Psychology
J. Neural. Trans.	Journal of Neural Transmission
J. Neuro. Psychiatry Clin. Neurosci.	The Journal of Neuropsychiatry and Clinical Neuroscience
J. Neurol	The Journal of Neurology
J. Neurosci.	Journal of Neuroscience
Mol. Cell. Biol.	Molecular and Cellular Biology
Mutat. Res.	Mutation Research
Nat. Genet.	Nature Genetics
Neurobiol. Dis.	Neurobiology of Disease
Proc. Natl. Acad. Sci.	Proceedings of the National Academy of Sciences

References

- Alves, G.S., O'Dwyer, Jurcoane, A., Knochel, V.O., Knochel, C., Prvulovic, D., Sudo, F., Alves, C.E., Valente, L., Moreira, D., Fuber, F., Karakaya, T., Panel, J., Engelhardt, E., Laks, J. 2012. Different patterns of white matter degeneration using multiple diffusion indices and volumetric data in mild cognitive impairment and Alzheimer patients. *PLoS ONE*. 7(12), e52859.
- Beauquis, J., Pavia, P., Pomilio, C., Vinuesa, A., Podlutskaya, N., Galvan, V., Saravia, F. 2013. Environmental enrichment prevents astroglial pathological changes in the hippocampus of APP transgenic mice, model of Alzheimer's disease. *Experimental Neurology*. 239, 28-37.
- Becker, J.A., Hedden, T., Carmasin, J., Maye, J., Rentz, D.M., Putcha, D., et al., 2011. Amyloid-B associated cortical thinning in clinically normal elderly. *Ann. Neurol*. 69, 1032-1042.
- Borgesius, N.Z., de Waard, M.C., van der Pluijm, I., Omrani, A., Zondag, G.C.M., van der Horst, G.T.J., Melton, D.W., Hoeijmakers, J.H., Jaarsma, D., Elgersma, Y. 2011. Accelerated age-related cognitive decline and neurodegeneration, caused by deficient DNA repair. *The Journal of Neuroscience*. 31(35), 12543-12553.
- Braak, H., Del Tredici, K., Bratzke, H., Hamm-Clement, J., Sandmann-Keil, D., Rub, U. 2002. Staging of the intracerebral inclusion body pathology associated with idiopathic Parkinson's disease (preclinical and clinical stages). *J. Neurol.*, 249 (suppl. 3), III/1-5.
- Buchman, A.S., Nag, S., Shulman, J.M., Lim, A.S.P., VanderHorst, V.G.J.M., Leurgans, S.E., Schneider, J.A., Bennett, D.A. 2012. Locus Coeruleus neuron density and Parkinsonism in older adults without Parkinson's disease. *Movement Disorders*. 000, 1-7.
- Butt, F.M.A., Moshi, J.R., Owibingire, S., Chindia, M.L. 2010. Xeroderma Pigmentosum: a review and case series. *Journal of Cranio-Maxillo-Facial Surgery*. 38, 534-537.
- Chang, S., Jung, I., Han, G., Kim, N., Kim, H., Kim, C. 2013. Proteomic profiling of brain cortex tissues in Tau transgenic mouse model of Alzheimer's disease. *Biochemical and Biophysical Research Communications*. 430, 670-675.
- Chen, H., Zhang, S., Hernan, M., Willett, W., Ascherio, A. 2003. Weight loss in Parkinson's disease. *Ann Neurol*. 53, 676-679.

de Graaf, E.L., Vermeij, W.P., de Waard, M.C., Rijksen, Y., van der Pluijm, I., Hoogenraad, C.C., Hoeijmakers, J.H.J., Altelaar, A.F.M., Heck, A.J.R. 2013. Spatio-temporal analysis of molecular determinants of neuronal degeneration in the aging mouse cerebellum. MCP papers, M112.024950.

de Waard, M.C., van der Pluijm, I., Borgesius, N.Z., Comley, L.H., Haasdijk, E.D., Rijksen, Y., Ridwan, Y., Zondag, G., Hoeijmakers, J.H.J., Elgersma, Y., Gillingwater, T.H., Jaarsma, D. 2010. Age-related motor neuron degeneration in DNA repair-deficient Ercc1 mice. *Acta Neuropathologica*. 120: 461-475.

Dolle, M. E.; Busuttil, R. A.; Garcia, A. M.; Wijnhoven, S.; van Drunen, E.; Niedernhofer, L. J.; van der Horst, G.; Hoeijmakers, J. H.; van Steeg, H.; Vijg, J. Increased genomic instability is not a prerequisite for shortened lifespan in DNA repair deficient mice. *Mutat. Res.* **2006**, 596 (1-2), 22–35.

Eller, M., Williams, D. R., 2011. α -Synuclein in Parkinson's disease and other neurodegenerative disorders. *Clinical Chemistry and Laboratory Medicine*. 49.3: 403-408.

Gerhard, A., Pavese, N., Hotton, G., Turkheimer, F., Es, M., Hammers, A., Eggert, K., Oertel, W., Banati, R.B., Brooks, D.J., 2006. In vivo imaging of microglial activation with [11C] (R)-Pk11195 PET in idiopathic Parkinson's disease. *Neurobiol. Dis.* 21., 404-412.

Ghosh, A., Kanthasamy, A., Joseph, J., Anantharam, V., Srivastava, P., Dranka, B., Kalyanaraman, B., Kanthasamy, A. 2012. Anti-inflammatory and neuroprotective effects of an orally active apocynin derivative in pre-clinical models of Parkinson's disease. *Journal of Neuroinflammation*. 9:241

Ghosh, A., Roy, A., Matras, J., Brahmachari, S., Gendelman, H.E., Pahan, K. 2009. Simvastatin inhibits the activation of p21^{ras} and prevents the loss of dopaminergic neurons in a mouse model of Parkinson's disease. *J. Neurosci.* 29(43):13543-13556.

Glass, C.K., Saijo, K., Winner, B., Marchetto, M.C., Gage, F.H. 2010. Mechanisms underlying inflammation in neurodegeneration. *Cell* 140, 918-934

Goss, J.R., Beer-Stolz, D., Robinson, A.R., Zhang, M., Arbutas, N., Robbins, P.D., Glorioso, J.C., Niedernhofer, L.J. 2011. Premature aging-related peripheral neuropathy in a mouse model of progeria. *Mechanisms of Ageing and Development*. 132, 437-442.

Grand'Maison, M., Zehntner, S.P., Ho, M., Hebert, F., Wood, A., Carbonell, F., Zijdenbos, A.P., Hamel, E., Bedell, B.J. 2013. Early cortical thickness changes

predict b-Amyloid deposition in a mouse model of Alzheimer's disease. *Neurobiology of Disease*. xxx, xxx-xxx.

Hamilton, M.L., Van Remmen, H., Drake, J.A., Yang, H., Guo, Z.M., Kewitt, K., Walter, C.A., Richardson, A. 2001. Does oxidative damage to DNA increase with age? *98(18)*, 10469-10474.

Heneka, M.T., O'Banion, M.K., Terwel, D., Kummer, M.P. 2010. Neuroinflammatory processes in Alzheimer's disease. *J Neural Transm.*117, 919-947.

Jin, K., Peel, A.L., Mao, X.O., Xie, L., Cottrell, B.A., Henshall, D.C. & Greenberg, D.A. (2004b) Increased hippocampal neurogenesis in Alzheimer's disease. *Proc. Natl. Acad. Sci. USA*, 101, 343–347.

Kaup, A.R., Mirzakhani, H., Jeste, D.V., Eyler, L.T. 2011. A review of the brain structure correlates of successful cognitive aging. *J Neuropsychiatry Clin Neurosci.* 23(1), 6-15.

Lazarov, O. & Marr, R.A. (2010) Neurogenesis and Alzheimer's disease: at the crossroads. *Exp. Neurol.*, 223, 267–281.

McGeer, P.L., Itagaki, S., Boyes, B.E., McGeer, E.G., 1988. Reactive microglia are positive for HLA-DR in the substantia nigra of Parkinson's and Alzheimer's disease brains. *Neurology* 38, 1285-129

McNeil, E.W., Melton, D.W. 2012. DNA repair endonuclease ERCC1-XPF as a novel therapeutic target to overcome chemoresistance in cancer therapy. *Nucleic Acids Research.* 40 (20), 9990-10004.

McWhir, J.; Selfridge, J.; Harrison, D. J.; Squires, S.; Melton, D. W. Mice with DNA repair gene (ERCC-1) deficiency have elevated levels of p53, liver nuclear abnormalities and die before weaning. *Nat. Genet.* **1993**, 5 (3), 217–224.

Nevedomskaya, E., Meissner, A., Goral, S., de Waard, M., Ridwan, Y., Zondag, G., van der Pluijm, I., Deelder, A.M., Mayboroda, O.A. 2010. Metabolic profiling of accelerated aging ERCC1^{del} mice. *Journal of Proteome Research.* 9, 3680-3687.

Niedernhofer, L.J., Odijk, H., Budzowska, M., van Drunen, E., Maas, A., Theil, A.F., de Wit, J., Jaspers, N.G.J., Beverloo, H.B., Hoeijmakers, J.H.J. et al.. (2004) The structure-specific endonuclease Ercc1-Xpf is required to resolve DNA interstrand cross-link-induced double-strand breaks. *Mol. Cell. Biol.*, 24, 5776–5787

Niedernhofer, L.J., Garinis, G.A., Raams, A., Lalai, A.S., Robinson, A.R.,

Appeldoorn, E., Odijk, H., Oostendorp, R., Ahmad, A., van Leeuwen, W. et al. (2006) A new progeroid syndrome reveals that genotoxic stress suppresses the somatotroph axis. *Nature*, 444, 1038–1043.

Pievani, M., Bocchetta, M., Boccardi, M., Cavedo, E., Bonetti, M., Thompson, P.M., Frisoni, G.B. 2013. Striatal Morphology in early-onset and late-onset alzheimer's disease: a preliminary study. *Neurobiology of Aging*, xxx, 1-12.

Pradhan, S., Andreasson, K. 2013. Commentary: Progressive inflammation as a contributing factor to early development of Parkinson's disease. *Experimental Neurology*. 241, 148-155.

Secher, M., Andrieu, S., Gillette-Guyonnet, S., Soto, M., Rolland, Y., Cantet, C., Vellas, B., Ritz, B., the REAL.fr group. 2012. Weight changes in Alzheimer's disease patients with increased aberrant motor behavior. *Int J Geriatr Psychiatry*.

Sharma, J., Turton, J. 2012. Olfaction, dyskinesia and profile of weight change in Parkinson's disease: Identifying neurodegenerative phenotypes. *Parkinsonism and Related Disorders*. 18, 964-970.

Teipel, S., Bayer, W., Alexander, G.E., Zebuhr, Y., Teichberg, D., Kulic, L., Schapiro, M., Moller, H., Rapoport, S.I., Hampel, H. 2002. Progression of Corpus callosum atrophy in Alzheimer disease. *Arch Neurol*. 59, 243-248.

Tsodikov, O.V., Enzlin, J.H., Schärer, O.D. and Ellenberger, T. (2005) Crystal structure and DNA binding functions of ERCC1, a subunit of the DNA structure-specific endonuclease XPF-ERCC1. *Proc. Natl Acad. Sci. USA*, 102, 11236–11241.

Vegh, M.J., de Waard, M.C., van der Pluijm, I., Ridwan, Y., Sassen, M.J.M., van Nierop, P., van der Schors, R., Li, K.W., Hoeijmakers, J.H.J., Smit, A.B., van Kesteren, R.E. 2012. Synaptic proteome changes in a DNA repair deficient ERCC1 mouse model of accelerated aging. *Journal of Proteome Research*. 11, 1855-1867.

Winner, B., Kohl, Z., Gage, F.H. 2011. Neurodegenerative disease and adult neurogenesis. *European Journal of Neuroscience*. 33, 1139-1151.

Zussy, C., Brureau, A., Keller, E., Marchal, S., Blayo, C., Delair, B., Ixart, G., Maurice, T., Givalois, L. 2013. Alzheimer's disease related markers, cellular toxicity and behavioral deficits induced six weeks after oligomeric Amyloid-B injection in rats. *PLoS ONE*. 8(1).e53117.

Vita

[REDACTED]

[REDACTED]

[REDACTED]

[REDACTED]

[REDACTED]

[REDACTED]

[REDACTED]

[REDACTED]

[REDACTED]

[REDACTED]

[REDACTED]

[REDACTED]

[REDACTED]

[REDACTED]

[REDACTED]

[REDACTED]

[REDACTED]

[REDACTED]

- 1. [REDACTED]
- 2. [REDACTED]
- 3. [REDACTED]

[REDACTED]

- 1. [REDACTED]
- 2. [REDACTED]

[REDACTED]

- 1. [REDACTED]
- 2. [REDACTED]

[REDACTED]

█ [REDACTED]

█ [REDACTED]

[REDACTED]

[REDACTED]

█ [REDACTED]

[REDACTED]

[REDACTED]

[REDACTED]

█ [REDACTED]

